Il seguente lavoro è stato pubblicato sulla rivista Sensors and Actuators B: Chemical, con DOI: 10.1016/j.snb.2015.02.033

Graphene and ionic liquids new gel paste electrodes for caffeic acid quantification

Federica Valentini[a,*], Davide Roscioli[a], Marilena Carbone[a], Valeria Conte[a], Barbara Floris[a], E.M. Bauer[b], Nicoletta Ditaranto[c], Luigia Sabbatini[c], E. Caponetti[d,e], D. Chillura-Martino[d]

[a]Dipartimento di Scienze e Tecnologie Chimiche, Via della Ricerca Scientifica 1, 00133 Rome, Italy

[b]Istituto di Struttura della Materia del Consiglio Nazionale delle Ricerche (ISM-CNR), RM 1, Via Salaria km 29.3, 00015 Monterotondo, Italy

[c]Dipartimento di Chimica, Università degli Studi di Bari "Aldo Moro", via Orabona 4, 70125 Bari, Italy

[d]Centro Grandi Apparecchiature, University of Palermo, Via F. Marini 14, 90128 Palermo, Italy[e]Department of Physical Chemistry, University of Palermo, Viale delle Scienze 90128 Palermo, Italy

abstract

Graphene/ionic liquids nanocomposite gels were synthesized by an electrochemical etching approachand fully characterized under a morphological and structural point of view. For this purpose,several analytical techniques were applied, as HR-TEM/EDX (High Resolution-Transmission Elec-tron Microscopy/Energy Dispersive X-Ray Analysis); FE-SEM/EDX (Field Emission-Scanning ElectronMicroscopy/Energy Dispersive X-Ray Analysis); XPS (X-Ray Photoelectron Spectroscopy); FT-IR (FourierTransform-Infrared Spectroscopy) and electrochemical techniques. After the characterization study,nanocomposite-gel paste electrodes were assembled, exhibiting a selective and specific detectiontoward the caffeic acid oxidation. Better performances in terms of linear range of concentration (from0.025 to 2.00 M), reproducibility (intra-; 1.40% and inter-electrode reproducibility-3.20%), sensitivity(3389/ A mM−1cm−2), fast response time (2 s) and detection limit (0.005 mM) were obtained, in compar-ison with other chemically modified electrodes, described in literature for the caffeic acid detection. Thisnanocoposite-gel could represent a new prototype of miniaturized nanostructured sensors useful for the"in situ" quantification of an important molecule, having pharmacological properties, anti-inflammatory,antibacterial, antiviral, immunomodulatory and antioxidant effects.

Introduction

The Single Layer of Graphene (SLG) and Few Layer Graphene(FLGs) derivatives represent new interesting nanostructured mate-rials for their countless chemical–physical and mechanical features[1]. The properties of the new nanomaterials are strictly relatedto the surface chemistry and therefore to the oxygen con-taining functionalities [2,3]. The surface modification and theselective functionalization/engineering of graphene sheets dependon the synthesis route [3] used for nanographene production.Recently, the exfoliation process of a graphite anode into graphenenanosheets, triggered by anodic oxidation of water in presence oflonic Liquids (ILs) has been reported [4]. It is very well knownin the literature [4] that water is one of the key factors that significantly affect several properties of ILs, such as viscosity,electrochemical potential window and conductivity [4]. Especiallythe electrochemical conductivity is proportional to the specificdouble layer capacitance (CDL) of the electrodic materials, theirspecific surface area (SSA), and to the accessible surface portion(the electrochemical area, related to the roughness of the work-ing electrode surfaces) for electrolytes and electro-active moleculartargets [5]. In this communication, two different nanocompos-ite gels were electrochemically synthesized as G/bmim+Br−andG/bmim+Cl−. Among several kind of ILs described in literature,bmim+Cl−and bmim+Br−have been selected because they exhibitssuperior chemical-physical and electrochemical properties (TableS1A and B in ESI), especially in terms of higher electrochemical andelectronic conductivity, wider potential window and lower viscos-ity (this latter related to the mobility of the charged ions, duringthe electron transfer processes that occur in the solution duringthe CV and DPV measurements). The second reason concerning thechoice of these two kinds of ILs is related to our previous work, [5b] where we studied the influences of different cations in ILs compo-sition (maintaining constant the same anion component) on theelectrochemical signals and here, we are interested to investigatethe influence of different anions on the sensor responses. Finallywe selected the two ILs for their biocompatibility [5a,b] if com-pared with that exhibited from other ILs, reported in Table S1B,ESI. The resulting new nanocomposite materials show an excep-tionally high SSA (2700 m2/g, evaluated in this work) and also a highelectrochemical conductivity (reported in ESI). These data suggestthat G/ILs nanocomposite gels represent eligible new nanomate-rials for the assembly of electrodes and electrochemical devices.Accordingly, in the present communication we describe the use ofG/ILs based paste electrodes for a selective amperometric detec-tion of caffeic acid; an important target molecule that exhibits(as flavonoids and phenolic compounds [6]) several pharmacolog-ical properties, such as antiproliferative activity in human tumorcells [7], or anti-inflammatory [8], antibacterial [9], antiviral [10],immunomodulatory [11] and antioxidant [12] effects. A morpho-logical/topographic investigation (performed by HR-TEM/EDAX:High Resolution-Transmission Electron Microscopy/Energy Dispersive X-Ray Analysis) and a structural study (carried out by the XPS:X-Ray Photoelectron Spectroscopy and FT-IR: Fourier Transform-Infrared spectroscopy) were performed, prior to examining theanalytical performance of the resulting sensor in caffeic acid oxidation.

2. Experimental

All the materials and reagents were reported in ESI.

2.1. Apparatus and procedures

2.1.1. HR-TEM/SAED

HR-TEM analyses was performed on G/bmim+Cl− nanocom-poite gel. A JEM-2100 (JEOL, Japan) microscope was used, operatingat 200 kV accelerating voltage and equipped with an energy disper-sive X-ray spectrometer (EDS) (Oxford Instruments, UK) suited forelement identification. The acquired high-resolution micrographswere obtained by the Inverse Fast Fourier Transformer (IFFT),equipped by the Digital-Micrograph GATAN software. The sampleswere prepared by placing a drop of G/bmim+Cl− nanocompoite gelon a copper grid and letting it dry.

2.1.2. FE-SEM/EDAX(Field Effect-Scanning electron Microscopy/Energy Dispersive X-Ray Analysis).

The topographic characterization of the modified SPE (Screen Printed Electrodes) surfaces was performed by using a field emission-scanning electron microscope/energy dispersive X-ray analyzer (FE-SEM/EDX, LEO 1550) equipped with a sputter coater (Edwards Scan Coat K550X). A volume of 5 _L of the dispersions has been directly deposited on the SPE surface, leaving the solvent to evaporate at room temperature (RT). The modified SPEs were fixed on the aluminum stub, with carbon tape. The samples were then coated by a thin Au layer (with a thickness of 20 nm),deposited by sputtering for 2 min at I = 25 mA.

2.1.3. XPS. (X-ray photoelectron spectroscopy)

The surface characterization of ionic liquids and graphene modified gels was performed by using a Thermo VG Theta Probe spectrometer equipped with a microspot monochromatised AlK _source (spot = 300 _m). Survey spectra were recorded in constant analyzer energy mode (CAE) at a pass energy of 150 eV, while high-resolution regions (C1s, O1s, N1s) were acquired in CAE mode at a pass energy of 100 eV. When charging compensation was required a flood gun operating at − 1 eV was used. Calibration of the Binding Energy (BE) scale was performed by fixing the C C component at BE values of 284.8 ± 0.1 eV. The samples were spin coated on glass substrates and directly fixed on the XPS sample holder with car-bon tape. The base pressure during the analyses was in the range10^{-9}mbar.

2.1.4. FT-IR (Fourier transform-infra red spectroscopy)

The spectrophotometer that was used in this study is a ShimadzuPrestige-21, as equipment model, having these set-up experimental parameters: the resolution of 4 $cm^{-1}$and the wavenumber range of 4000–400 cm^{-1}. The liquid samples have been sandwiched between NaCl disks.

2.1.5. Pore surface area measurements (BET method)

Nitrogen adsorption was measured at 77 K with an automatic adsorptiometer (Micrometrics ASAP2000). The samples were pre-treated at 573 K for 2 h under vacuum. The surface areas were determined from adsorption values for five relative pressures (P/P_0)ranging from 0.05 to 0.2 using the BET method [13]. The pore volumes were determined from the total amount of N_2 adsorbed between P/P_0= 0.05 and P/P_0= 0.98.

2.1.6. Electrochemical measurements.

The electrochemical cell was assembled with a conventional three-electrode system: a G/bmim+Cl−; G/bmim+Br− based paste electrodes (PEs) working electrode (1-mm diameter), a Ag/AgCl/KCl(3M) reference electrode, and a Pt counter electrode. All experiments were carried out at room temperature. Cyclic voltammetry experiments were carried out at a scan rate of 100 mV/s over the relevant potential range using 0.1 M phosphate buffer (pH 7.4). The value of 100 mV/s represents the best compromise to achieve a higher Signal/to Noise Ratio, during measurements. It was selected during the scan rate study, performed by CV, ranging from 5 mV/s to 500 mV/s, as scan rate. DPV were performed with a pulse amplitude of 50 mV, a pulse width of 60 ms, a scan rate of 10 mV/s, a pulse interval of 200 ms, and a sampling time of 20 ms; E_i= − 0.2 Vand E_f= +0.8 V for the caffeic acid calibration curves. Only for the AA, 0.1 M acetate buffer (pH = 5.4) and a scan rate 100 mV/s have been used as additional working conditions, according to the literature [14a]. The electrochemical and physiochemical properties of carbon based materials used for the paste electrodes assembly, such as: the specific double layer capacitance (CDL) of the electrode materials, their specific surface area (SSA) and the electrical resistivity were evaluated according to the literature, and reported in Table S1-A, in ESI section. For a comprehensive discussion see Ref.[14b, and references cited therein]. The permeability (P%) test and the perm-selectivity assay were described in ESI, in details.

2.2. Synthesis of materials and paste electrodes assembly

2.2.1. Ionic liquids synthesis & NMR characterization.

The syntheses were performed in water, slightly modifying a literature method [15]. 1-Butyl-3-methylimidazolium bromide, bmim+Br−. 70 ml distilled H_2O and 60 ml 1-methylimidazole were mixed under a gentle stream of Ar. 1-Bromobutane (162 ml,2 equivalents) was added dropwise, under argon atmosphere, and the resulting mixture was stirred ad 70 ◦ C in a thermostat-ted oil bath. After 24 h, the $CuCl_2$test for the presence of1-methylimidazole was negative and therefore the reaction was stopped, cooled and transferred into a separatory funnel. After removing the organic phase (alkyl bromide excess), the aqueous layer was repeatedly extracted with diethyl ether, to remove 1-bromobutane completely. After treatment with active carbon, to remove yellow impurities, the solution was poured into a 250 mlErlenmeyer flask and diluted with more water. The title was deter-mined lyophilizing a 5 ml sample and weighing the white solid bmim+Br−. Yield, 93.5%.1H NMR spectrum of bmim+Br−in CDCl3: H (300 MHz, CDCl3): 10.6 (s, 1H, H-2); 7.58 (s, 1H, H-5); 7.43 (s,1H, H-4); 4.27 (t, 2H, CH2); 4.06 (s, 3H, CH3); 1.9 and 1.4 (m,4H, CH2); 1 (t, 3H, CH3). The corresponding spectrum (Fig.S1) is reported on ESI section. 1-butyl-3-methylimidazolium chloride [bmim+]Cl−was obtained with the same procedure, at 85 ◦ C,because of the low reactivity of 1-chlorobutane. However, after 10days 1-methylimidazole was still present. Only after adding a third equivalent of 1-chlorobutane and raising the temperature to 90 ◦ C,the reaction was complete after additional 24 h. Yield, 83%. Structure and purity were determined by1H NMR spectrum.1H NMR spectrum of bmim+Cl−in

CDCl3: H (300 MHz, CDCl3): 10.6 (s, 1H,H-2); 7.58 (s, 1H, H-5); 7.43 (s, 1H, H-4); 4.27 (t, 2H, CH2); 4.06(s, 3H, -CH3); 1.9 and 1.4 (m, 4H, CH2); 0.9 (t, 3H, CH3-4). The corresponding spectrum (Fig. S2) is reported on ESI section.

2.2.2. G/ILs nanocomposites synthesis and paste electrode assembly

Electrochemical exfoliation. Nanocomposite gels were synthesized according to the literature [16,17]. The anodic etching of the graphite working electrode was performed in a IL electrochemical bath, applying a static potential bias between two graphite rods, that act as working and reference electrodes, respectively. The exfoliation mechanism from the graphite electrode toward the functionalized multi-layers of graphene is due to a complex reaction mechanism based on the anodic oxidation of water and anionic intercalation from ILs (these later synthesized in Tor Vergata Uni-versity, according to the experimental procedures described above, in Section 2.2).

2.2.3. Paste electrode assembly.

The G/ILs paste electrodes used for the quantitative electro-chemical detection of caffeic acid were prepared hand-mixing in a mortar the nanocomposite gels and then packed the resulting paste into a cavity (1 mm diameter; 1 mm depth) at the end of the Teflon tube. The electrical contact was provided by a copper wire connected to the nanocomposite gel paste electrode in the inner hole of the tube. The nanocomposite gel paste was stored at R. T.in desiccators until used. Carbon paste electrodes and also Glassy Carbon paste electrodes, used for comparison, were assembled ina similar way using micrometric Graphite powder, Glassy Carbon powder, respectively, and mineral oil in the same ratio of 80:20%(w/w%), according to our previous paper [14(a)]. The surfaces of the resulting nanocomposite gel paste electrodes were carefullysmoothed and rinsed carefully with double-distilled water prior to use for measurements.

3. Results and discussion

3.1. Morphological and structural characterization of the electrode materials

In Fig. 1(a) the TE micrograph of the G/bmim+Cl− gel is reported. The nanocomposite aggregates have an irregular shape. From the degree of transparency it can be inferred that the number of layers is less than 10. This is also confirmed by the Selected Area Electron Diffraction (SAED) reported in Fig. 1(b), which shows the typical hexagonal crystal lattice of the aggregates. The G/ILs nanocomposite gels were also characterized by X-ray photoelectron spectroscopy (XPS). In particular, the comparison between nitrogen spectral region (N1s) of both ILs and gels proved to be diagnostic to gain information on their chemical interactions. The spectra are reported in Fig. 2 where the overlap of nitrogen signals of each IL (red line) with the corresponding G/IL (green line) is shown. The nanocomposite gels are characterized by more components in the lower binding energy (BE) region. The N1s curve-fitted signals (insets of Fig. 2) showed the peak at BE = 401.4 ± 0.1 eV and the peak at BE = 399.3 ± 0.7 eV, attributed to N+ and N–C of imidazolium ring, respectively. A third component is also present atBE = 400.3 ± 0.4 eV, indicating an energy shift due to a chemical interaction of the ILs with the graphene sheets. The charge trans-fer between conjugated aromatic rings and the functionalization groups is already reported [18]; a similar effect can be invoked in the nanocomposites studied in this paper. The interactions via the acidic hydrogen of imidazolium ring and the mesomeric effect of graphene planes influence the BE of the nitrogen atoms of bmim+Br−and bmim+Cl−: the resonance on the ring is hindered, thus resulting in the three component peaks. The infrared spectra of pure bmim+Cl− and nanocomposite G/bmim+Cl−gel are shown in Fig. 3 (and also Fig. S6, in ESI)and both are heavily influenced by the presence of water [19].In fact, the spectral region above 3000 cm−1is strongly influenced by typical OH stretching vibrations covering all the other peaks, especially in the case of pure bmim+Cl−. The nanocomposite G/bmim+Cl−gel shows a sharper OH stretching vibration centered around 3450 cm−1probably due to a different nature ofO H and/or hydrogen bonds. In each case the presence of water is confirmed in both samples by the OH bending vibration located at ca. 1645 cm−1. Surprisingly, the nanocomposite gel G/bmim+Cl− material shows also peaks at 1700 cm−1and 1735 cm−1, normally ascribed to the presence of carbonyl groups (C O stretching) [20]. The latter functional group may be the reason for the different peak shape of the previously described OH stretching vibration inthis sample. FT-IR spectra of the nanocomposite gel shows two broad peaks above 3000 cm−1, i.e. 3145 and 3050 cm−1, ascribed to stretching vibrations of C H bonds in the imidazole ring andN CH3group [21]. CH2and CH3symmetric and asymmetric stretching of the butyl chain can be observed in both samples inthe spectral region 2855–2965 cm−1. Special attention should be deserved to characteristic bands of the imidazolium ring locatedat approximately 1570 cm−1, 1460 cm−1and 1170 cm−1. The latter bands are slightly shifted toward lower wavenumbers in the exfoli-ated G/bmim+Cl−sample (2–5 cm−1), as expected for − stacking interactions between the imidazolium rings and the conjugation ofgraphene sheets [22].

3.2. Electro-analytical characterization of the chemically modified sensors

The G/ILs nanocomposite gels were used for the assembly of paste electrodes-G/ILs-PEs (see Fig. 4a and b) in order to test the electron-transfer properties of these new nanostructured mate-rials, in presence of several electro-active targets. FE-SEM/EDAX micrographs (Fig. 5) reveal a more homogeneous and uniform morphology of the resulting G/bmim+Cl−-PEs, when compared with that exhibited by the conventional micrometric graphite carbon paste electrodes-CPE, Glassy Carbon Paste Electrodes-GCPE and also G/bmim+Br−-PEs (Fig. 5a–d). In addition, an enhancement of the crystalline structure was also observed in presence of the G/ILs-PEs (as confirmed by the XRD spectra, data not shown here). The morphology strongly influences the electron-transfer processes of the electro-active molecular probes (see Fig. 5e–h in the same panel and Fig. S4 in ESI), from the bulk of the solution toward the electrode surfaces. For both G/ILs-PEs, the diffusion mechanism controls the electrochemical transfer in presence of [Ru(NH3)]6+reversible redox couple (Fig. S3, ESI) and other reversible and quasi-reversible molecular targets (summarized in Table 1, in the text).A detailed kinetic study, performed at different scan rate by CV(Cyclic Voltammetry) technique, demonstrates that the apparent heterogeneous first order electron-transfer kinetic constants (TableS2) indicate a performance of G/bmim+Cl−-PE better than those ofG/bmim+Br−-PE and of the conventional PEs described in literature(also reported in Table S2) and the conventional bare electrodes(also reported in Table S2 for comparison). The superior electro-chemical performances of the assembled G/bmim+Cl−-PE are also observed in presence of several different electro-active molecular targets, in terms of better I/A vs. V/E profiles and quantitative electrochemical parameters (all summarized in Table 1, in the full text).This trend might be explained considering that the electrochemical conductivity (i.e., the ionic mobility in solution) of the ILs, strictly depends on several parameters, such as: size, density, viscosity and diffusion coefficient. According to the literature [23–25], anions having larger size should show a lower viscosity and a higher diffusion coefficient. These effects would lead to a recombination of the cation and anion with formation of a neutral chemical species that does not contribute to the ionic conductivity in solution (whose performance depends on a combination of several different parameters, and

therefore it is difficult to predict). On the basis of the above results, a quantitative and selective DPV calibration of caffeic acid has been carried out by using the G/bmim+Cl−-PEs and G/bmim+Br−-PEs, as shown in Fig. 4c and d, Fig. 6a–c, respectively. Between the two assembled G/ILs−PEs, better analytical performances were observed in the case of the G/bmim+Cl−-PEs, especially in terms of sensitivity per unit of area, reproducibility (inter-; intra-reproducibility) and fast response time. The analytical features of G/bmim+Cl− PEs resulted superior also in comparison with other sensors described in literature and summarized in Table 2 but it exhibits a higher limit of detection (L.O.D.) and a lower sensitivity especially in comparison with the disposable biosensor based on platinum nanoparticles-reduced graphene oxide-laccase biocomposite for the determination of total polyphenolic content. The chemical sensor prototype, proposed here, presents an advantage if compared with the biosensor based on platinum nanoparticles-reduced grapheneoxide-laccase biocomposite that is the possibility to selectivelyrecognize only the caffeic acid. In addition, the higher selectivity ofthe analytical signal/response toward the oxidation of the caffeicacid, in presence of several common interferences (as AA, UA andAc, see Fig. 6 and Table 3) and also polyphenols and flavonoidscompounds (reported in Table 3) appears to be very promising forthe assembly of selective automatized electrochemical devices.In fact, high selectivity was achieved not only in presence ofthe standard interference models (as AA, UA and Ac) but also inpresence of a large number of polyphenols and flavonoids (as that investigated in Table 3 for the permeability and perm-selectivity test, evaluated according to our previous work [26]).An evaluation of the operational stability has been also carried out, in continuous working conditions (over 6 h) and the results(shown in ESI, in Fig. S5, where also a detailed description of the experimental procedures have been also reported) clearly demonstrated that the chemically modified sensors could be suitable for in situ measurements, to perform in real matrices (as food samples and pharmacological products), at least up to 6 h in continuous working conditions (recording a decrease of the original signal of≈30%. After 6 h the analytical signal significantly decreases over the50%, if compared with the initial value. Finally, taking into considerations the dimensions of the mod-ified paste electrodes by using graphene and ionic liquids gel nanocomposites, miniaturized and partially automatized electrochemical transducers could be assembled for several analytical applications, ranging from the food quality control, environment and biomedicine. This goal could be achieved controlling the “sur-face chemistry” of the graphene derivatives. According to the perm-selectivity data in Table 3, in order to testthe practical usefulness of the proposed platform a recovery study in real matrices has been also carried out (Table 4 and ESI for the experimental set-up applied for the recovery study). The recovery values of Caffeic acid at three different concentrations range from97.2 to 99.7%. The average recoveries of Caffeic acid is 98.8%. These results confirm the absence of matrices effects and the feasibility of using G/ILs/PEs for the Caffeic acid quantification in Plasma matrices. In addition, the excellent agreement with our electrochemical system and the reference HPLC chromatographic method (i.e. HPLC)for the Caffeic acid quantification contributes to validate the new analytical method, proposed inn this study.

4. Conclusions

In this work, new nano-gels, based on graphene and ionic liquids, were synthesized, characterized and used for the assembly of chemically modified carbon paste electrodes. The electron transfer processes and the corresponding heterogeneous kinetic constants were also investigated and, finally, the electrochemical reactivity toward caffeic acid was carried out. This alkaloid molecule was successfully detected with high sensitivity, excellent reproducibility and a fast response time.

References

[1] A.K. Geime, K.S. Novoselov, The rise of graphene, Nat. Mater. 6 (2007) 183.

[2] G. Goncalves, P.A.A.P. Marques, C.M. Granadeiro, H.I.S. Nogueira, M.K. Singh, J.Gracio, Surface modification of graphene nanosheets with gold nanoparticles: the role of oxygen moieties at graphene surface on gold nucleation and growth,Chem. Mater. 21 (2009) 4796.

[3] C.N.R. Rao, A.K. Sood, R. Voggu, K.S. Subrahmanyam, Some novel attributes ofgraphene, J. Phys. Chem. Lett. 1 (2010) 572.

[4] L. Jiong, J.-X. Yang, J. Wang, A. Lim, S. Wang, K.P. Loh, One-pot synthesis offluorescent carbon nanoribbons, nanoparticles, and graphene by the exfoliationof graphite in ionic liquids, ACS Nano 3 (2009) 2367.

[5] (a) A.J. Bard, L.R. Faulkner, Electrochemical Methods: Fundamentals and Appli-cations, Wiley & Sons, Inc., New York, 1980;(b) F. Valentini, D. Roscioli, M. Carbone, V. Conte, B. Floris, G. Palleschi, R. Flam-mini, E.M. Bauer, G. Nasillo, E. Caponetti, Oxidized graphene in ionic liquids forassembling chemically modified electrodes: a structural and electrochemicalcharacterization study, Anal. Chem. 84 (2012) 5823.

[6] P. Rapta, V. Misik, A. Stasko, I. Vrabel, Redox intermediates of flavonoids andcaffeic acid esters from propolis: an EPR spectroscopy and cyclic voltammetrystudy, Free Radic. Biol. Med. 18 (1995) 901.

[7] D.A. Smith, W. Banks, Biosynthesis, elicitation and biological activity ofisoflavonoid phytoalexins, Phytochemistry 25 (1986) 979.

[8] T. Brasseur, Anti-inflammatory properties of flavonoids, J. Pharm. Belg. 44(1989) 235.

[9] L. Guarini, Z.Z. Su, S. Zucker, J. Lin, D. Grunberger, P.B. Fisher, Growth inhibitionand modulation of antigenic phenotype in human melanoma and glioblastomamultiforme cells by caffeic acid phenethyl ester (CAPE), Cell. Mol. Biol. 38 (1992)513.

[10] G.-F. Wang, L.-P. Shia, Y.-D. Ren, Q.-F. Liu, H.-F. Liu, R.-J. Zhang, Z. Li, F.-H. Zhu,P.-L. He, W. Tang, P.-Z. Tao, C. Li, W.-M. Zhao, J.-P. g Zuo, Anti-hepatitis B virusactivity of chlorogenic acid, quinic acid and caffeic acid in vivo and in vitro,Antivir. Res. 83 (2009) 186.

[11] D.A. Smith, W. Banks, Biosynthesis, elicitation and biological properties ofisoflavanoid phytoalexins, Phytochemistry 25 (1986) 979.

[12] (a) W. Bors, M. Saran, Radical scavenging by flavonoid antioxidants, Free Radic.Res. Commun. 2 (1987) 289;(b) N. Darmon, Y. Fernandes, C. Cambon-Gros, S. Mutjavila, Quantification ofthe scavenger capacity of different flavonoids with regard to the superoxideion, Food Addit. Contam. 7 (1990) 60.

[13] S. Brunauer, P.H. Emmett, E. Teller, Adsorption of gases in multimolecular lay-ers, J. Am. Chem. Soc. 60 (1938) 309.

[14] (a) F. Valentini, A. Amine, S. Orlanducci, M.L. Terranova, G. Palleschi, Carbonnanotube purification: preparation and characterization of carbon nanotubepaste electrodes, Anal. Chem. 75 (2003) 5413;(b) A.G. Pandolfo, A.F. Hollenkamp, Carbon properties and their role in super-capacitors, J. Power Sources 157 (2006) 11.

[15] Y. Shen, Y. Zhang, D. Han, Z. Wang, D. Kuehner, L. Niu, Preparation of colorlessionic liquids on water for spectroscopy, Talanta 78 (2009) 805.

[16] L. Jiong, Y. Jia-Xiang, W. Junzhong, L. Ailian, W. Shuai, L. Kian Ping,One-pot synthesis of fluorescent carbon nanoribbons, nanoparticles, andgraphene by the exfoliation of graphite in ionic liquids, ACS Nano 3 (2009)2367.

[17] N.W. Pu, C.A. Wang, Y. Sung, Y.M. Liu, M.D. Ger, Production of few-layergraphene by supercritical CO2exfoliation of graphite, Mater. Lett. 63 (2009)1987.

[18] N. Liu, F. Luo, H.X. Wu, Y.H. Liu, C. Zhang, J. Chen, One-step ionic-liquid-assisted electrochemical synthesis of ionic-liquid-functionalized graphene sheets directly from graphite, Adv. Funct. Mater. 18 (2008) 1518.

[19] Y. Jeon, J. Sung, D. Kim, C. Seo, H. Cheong, Y. Ouchi, R. Ozawa, H. Hamaguchi,Structural change of 1-butyl-3-methylimidazolium tetrafluoroborate + watermixtures studied by infrared vibrational spectroscopy, J. Phys. Chem. B 112(2008) 923.

[20] G. Socrates, Infrared and Raman Characteristic Group Frequencies, John Wiley& Sons Ltd., 2001.

[21] M. Shukla, N. Srivastava, S. Saha, Theoretical and spectroscopic studies of1-butyl-3-methylimidazolium iodide room temperature ionic liquid: its dif-ferences with chloride and bromide derivatives, J. Mol. Struct. 975 (2010) 349.

[22] J. Im, S.D. Cho, M.H. Kim, Y.M. Jung, H.S. Kim, H.S. Park, Anomalous thermaltransition and crystallization of ionic liquids confined in graphene multilayers,Chem. Commun. 48 (2012) 2015.

[23] C. Chiappe, D. Pieraccini, Ionic liquids: solvent properties and organic reactivity,J. Phys. Org. Chem. 18 (2005) 275 (A Reviewer Commentary).

[24] (a) H.A. Every, A.G. Bishop, D. MacFarlane, G. Orädd, M. Forsyth, Transport prop-erties in a family of dialkylimidazolium ionic liquids, Phys. Chem. Chem. Phys.6 (2004) (1758);(b) M. Egashira, S. Okada, J.-I. Yamaki, N. Yoshimoto, M. Morita, Effect of smallcation addition on the conductivity of quaternary ammonium ionic liquids,Electrochim. Acta 50 (2005) 3708.

[25] S.-Y. Lee, H.H. Yong, Y.J. Lee, S.K. Kim, S. Ahn, Two-cation competition in ionic-liquid-modified electrolytes for lithium ion batteries, J. Phys. Chem. B 109(2005) 13663.

[26] A. Curulli, F. Valentini, S. Orlanduci, M.L. Terranova, G. Palleschi, Pt basedenzyme electrode probes assembled with Prussian Blue and conducting poly-mer nanostructures, Biosens. Bioelectron. 20 (2004) 1223.

[27] A.J. Wilkołazka, T. Ruzgas, L. Gorton, Use of laccase-modified electrode foramperometric detection of plant flavonoids, Enzyme Microb. Technol. 35(2004) 238.

[28] S.A.V. Eremia, I. Vasilescu, A. Radoi, S.-C. Litescu, G.-L. Radu, Disposablebiosensor based on platinum nanoparticles-reduced graphene oxide-laccasebiocomposite for the determination of total polyphenolic content, Talanta 110(2013) 164.

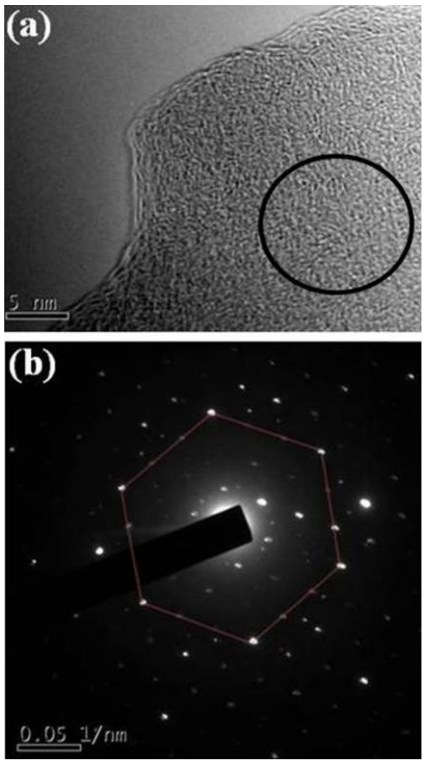

Fig. 1. (a) TEM images of G/bmim+Cl−nanocomposite gel (400,000×). (b) SAEDpattern of the area in the circle.

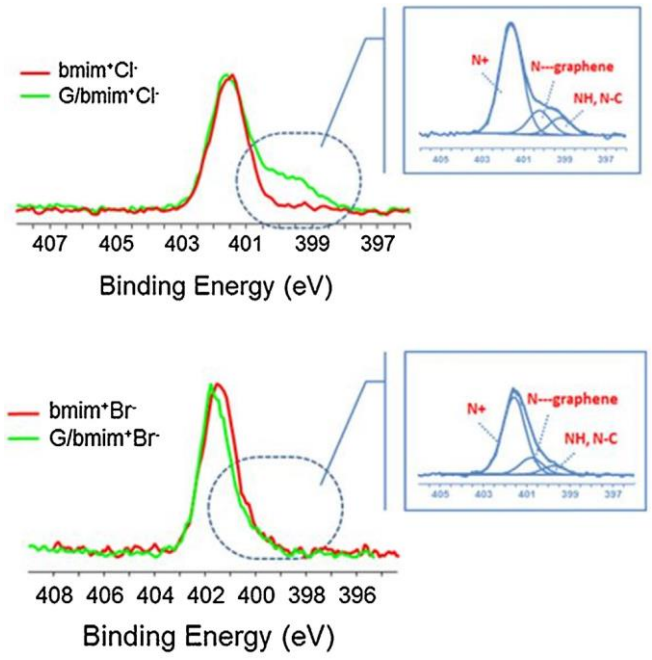

Fig. 2. N1s XP spectra of ILs and corresponding G/ILs generated by electrochemi-cal exfoliation in electrolyte with water content less than 10 wt%. In each panel, azoom showing the curve-fitted spectra of G/ILs nanocomposite gels, has also beenreported. (For interpretation of the references to color in text near the referencecitation, the reader is referred to the web version of this article.)

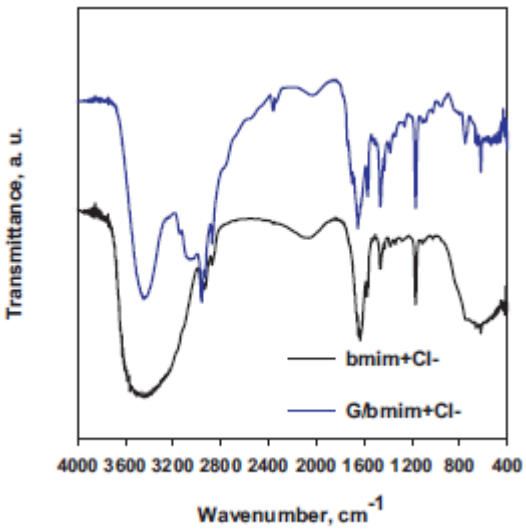

Fig. 3. FT-IR spectra of pure/native ionic liquids and G/ILs nanocomposite gels char-acterized in this work.

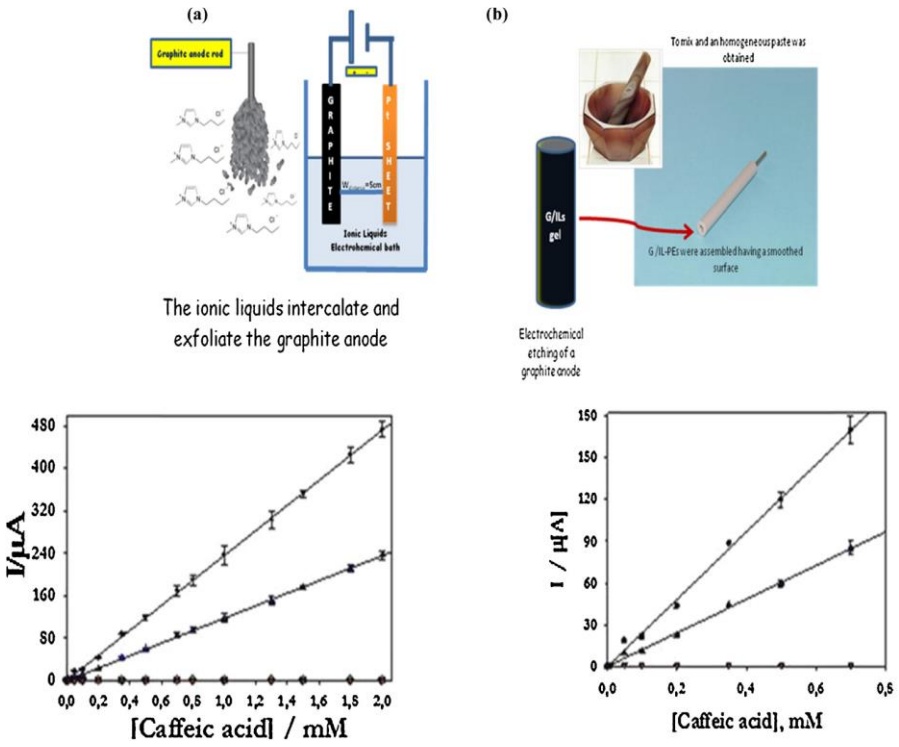

Fig. 4. (a) Scheme of the electrochemical anodic etching to synthesize the G/ILs based nano-gels. (b) Scheme of the assembly of the paste electrodes. (c) Calibration plotsperformed at G/bmim+Cl−-PEs ( ); G/bmim+Br−-PEs ( ); CPEs ( ); and GCPEs ( ). (d) Calibration plots at lowest concentration values, performed at G/bmim+Cl−-PEs ( );G/bmim+Br−-PEs ( ); CPEs ( ); and GCPEs ( ).

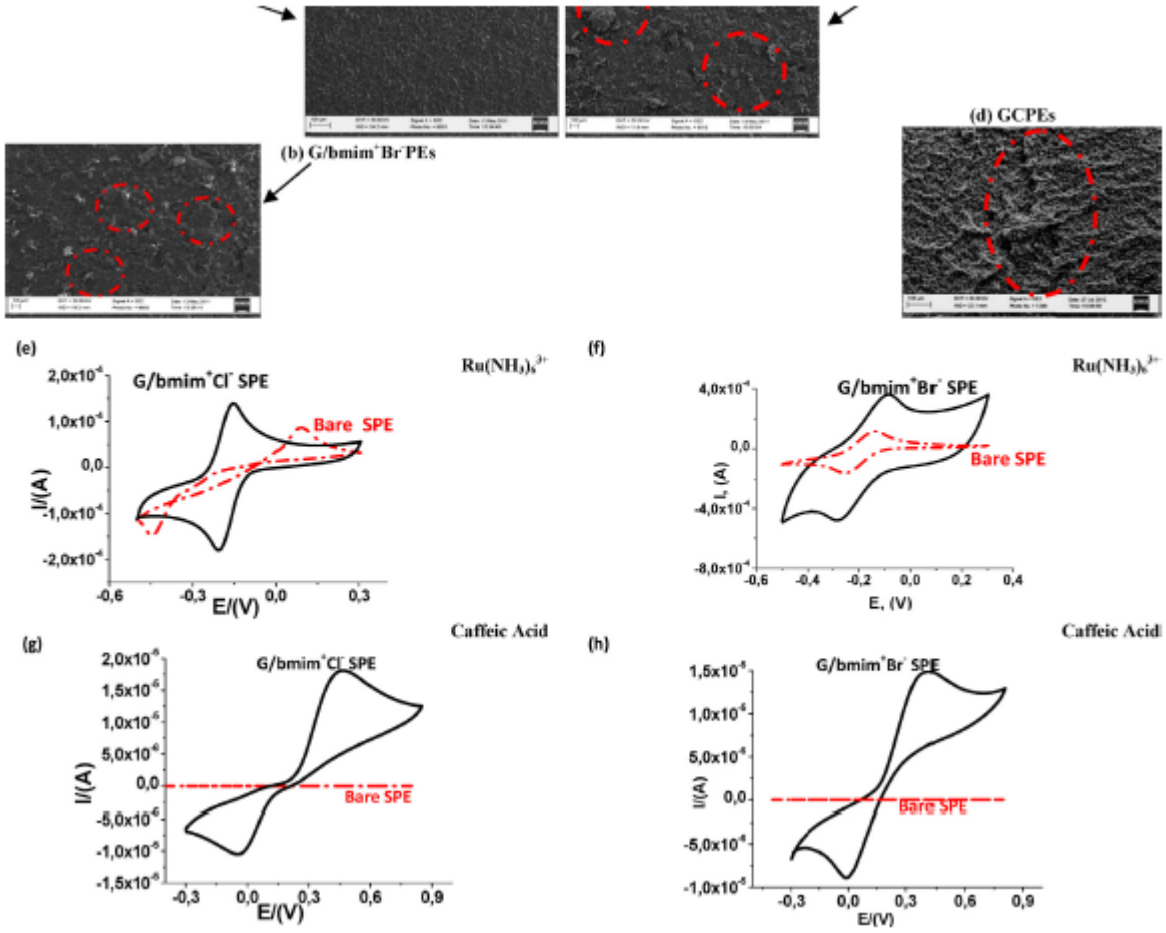

Fig. 5. (a) FE-SEM micrographs of the G/bmim+Cl−PE. (b) FE-SEM micrographs of the G/bmim+Br−PE, where the red circles indicate the gel nanocomposites detachment fromthe SPE surfaces. (c): FE-SEM micrographs of the typical reference CPE. (d): FE-SEM micrographs of the GCPE, where GC is not a solid electrode but is GC powder. (e) The CVplots of 1 mM of Ru (NH3)6Cl3, recorded at G/bmim+Cl−. (f) The CV plots of 1 mM of Ru (NH3)6Cl3, recorded at G/bmim+Br−. (g) 0.1 mM of caffeic acid, detected at G/bmim+Cl.(h) 0.1 mM of caffeic acid, detected at G/bmim+Br−. (For interpretation of the references to color in this figure legend, the reader is referred to the web version of the article.)

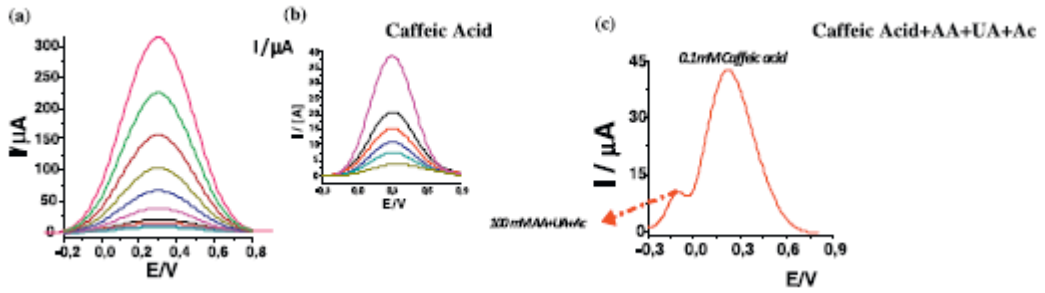

Fig. 6. (a) DPV calibration plot for caffeic acid, ranging from 2 mM (the outer line of the DPV graph) to 0.025 mM (the inner line in the same graph), performed at G/bmim+Cl−SPE. On the right corner, (b) The inset plot with the lowest concentration values (ranging from 0.025 mM to 0.1 mM) has been also reported, in the case of G/bmim+Cl−SPE.Finally in (c) a DPV calibration graph recorded at G/bmim+Cl−SPE in presence of 0.1 mM of caffeic acid and all the most common biological interferences (as AA, UA and Acat the concentration of 100 mM, in the same working solution), has been also shown.

Table 1
Electrochemical parameters obtained by CV, working at 100 mV/s.

Electro-active molecular targets	GCPE[b]	CPE	GPE/G-bmim$^+$Cl$^-$	GPE/G-bmim$^+$Br$^-$
$Fe(CN)_6^{3-}$ 1 mM	I_{pa}/I_{pc} = 1.50 ΔE_p = 500 mV	I_{pa}/I_{pc} = 2.50 ΔE_p = 765 mV	I_{pa}/I_{pc} = 1.00 ΔE_p = 95 mV	I_{pa}/I_{pc} = 2.00 ΔE_p = 198 mV
$Ru(NH_3)_6^{3+}$ 1 mM	I_{pa}/I_{pc} = 1.65 ΔE_p = 220 mV	I_{pa}/I_{pc} = 0.65 ΔE_p = 190 mV	I_{pa}/I_{pc} = 1.00 ΔE_p = 100 mV	I_{pa}/I_{pc} = 1.89 ΔE_p = 200 mV
Na_3IrCl_6-H_2O 1 mM	–	–	I_{pa}/I_{pc} = 1.05 ΔE_p = 62 mV	I_{pa}/I_{pc} = 1.49 ΔE_p = 201 mV
Ascorbic acid (AA)[a] 0.1 mM	I_{pa} = 2.50 μA E_{pa} = 540 mV	I_{pa} = 1.50 μA E_{pa} = 400 mV	–	–
Uric acid (UA) 0.1 mM	I_{pa} = 2.00 μA E_{pa} = 506 mV	I_{pa} = 2.90 μA E_{pa} = 386 mV	–	–
Acetaminophen (Ac) 0.1 mM	I_{pa} = 1.73 μA E_{pa} = 602 mV	I_{pa} = 1.90 μA E_{pa} = 672 mV	–	–
Caffeic acid 1 mM	I_{pa}/I_{pc} = 2.3 ΔE_p = 303 mV	I_{pa}/I_{pc} = 0.3 ΔE_p = 413 mV	I_{pa}/I_{pc} = 1.00 ΔE_p = 100 mV	I_{pa}/I_{pc} = 2.55 ΔE_p = 220 mV

[a] Only in presence of AA, different working conditions have been applied, as: 0.1 M acetate buffer pH = 5.4 and a scan rate of 100 mV/s. All the other electro-active molecular probes, the same working conditions have been applied, as: 0.1 M phosphate buffer (pH 7.4).
[b] GCPE: Glassy Carbon paste Electrodes.

Table 2
Quantitative calibration parameters obtained by DPV for this work.

Electrodes	References	Linear range of Concentration [mM]	Sensitivity per unit of area [μAmM^{-1}cm^{-2}]	Sensitivity [μAmM^{-1}]	Limit of Detection (L.O.D.) [mM]	RSD [%] Inter-electrodes N = 10 measurements	RSD[%] Intra–electrodes N = 3 measurements	Response time [s]
Laccase-modified electrodes	[27]	0.001–0.010	–	57.92	0.00056	–	–	–
C-SPE/Pt NPs/RGO	[28]	0.0002–0.002	–	2147	0.00009	–	–	60
GC Paste electrode (φ = 3 mm)	This work	0.020–0.050	0.0056	0.0004	0.020	13.40	10.60	18
CPaste electrodes (φ = 3 mm)	This work	0.025–0.10	0.2817	0.02	0.011	10.20	8.70	12
G/bmim$^+$Br$^-$ Paste electrodes (φ = 3 mm)	This work	0.025–2.00	1657	117.62	0.018	5.40	3.20	4
G/bmim$^+$Cl$^-$ Paste electrodes (φ = 3 mm)	This work	0.025–2.00	3389	240.63	0.005	3.20	1.40	2

Table 3
Permeability and perm-selectivity values [26], recorded at G/ILs/PEs, by DPV technique, following the experimental procedures reported in details, on ESI section.

Chemical compounds	Permeability [%] $P = I_{G/ILs/PEs}/I_{bare\,GPEs} \times 100$	Perm-selectivity $P_{Caffeic\ acid}/P_{interferent}$
Caffeic acid (Analyte)	100.0 ± 1.0	–
Ascorbic acid (Interferent)	1.9 ± 0.6	53.8
Uric acid (Interferent)	0.8 ± 0.1	120.5
Acetaminophen (Interferent)	0.2 ± 0.1	434.8
Coumaric acid (Interferent)	0.7 ± 1.1	137.0
Salycilic acid (Interferent)	0.3 ± 0.1	312.5
Protocatechuic acid (Interferent)	0.5 ± 0.2	217.4
Vanillic acid (Interferent)	1.0 ± 0.7	103.1
Gallic acid (Interferent)	1.2 ± 0.8	86.2
Syringing acid (Interferent)	0.3 ± 0.1	294.1
Quercetin (Interferent)	0.3 ± 0.1	322.6
Morin (Interferent)	0.2 ± 0.1	416.7
Rutinose Rutin (Interferent)	0.2 ± 0.1	454.6
Catechin (Interferent)	1.0 ± 0.8	103.1
(−)-Epicatechin (Interferent)	1.3 ± 0.9	74.6
Coumarin (Interferent)	1.0 ± 0.5	97.1
trans-Resveratrol (Interferent)	0.9 ± 0.7	114.9
Luteolin (Interferent)	0.2 ± 0.1	476.2
Cyanidin (Interferent)	0.8 ± 0.5	133.3
Chicoric acid (Interferent)	0.2 ± 0.1	416.7
Caffeoyltmalic acid (Interferent)	0.9 ± 0.2	114.9
Cholorogenic acid (Interferent)	0.4 ± 0.1	270.3

Table 4
Recoveries values for Caffeic acid in Plasma sample and the corresponding repeatability at different concentration of analyte. A comparative study, with the HPLC standard method, has been also reported.

Sample	Add (μM)	Found (μM)	Recovery (%)	RSD (%)	Water sample peak height by HPLC[a]	Plasma sample peak height By HPLC[a]	Recovery by HPLC[a] (%)
Plasma	25	24.3	97.2	1.3	43,733	42,865	98.0
	50	49.8	99.6	0.8	87,467	87,089	99.6
	100	99.7	99.7	0.5	17,4934	174,879	100

[a] For the experimental details see ESI.